

This article was downloaded by: [130.132.123.28]

On: 13 July 2015, At: 22:28

Publisher: Taylor & Francis

Informa Ltd Registered in England and Wales Registered Number: 1072954 Registered office: 5 Howick Place, London, SW1P 1WG



Journal of Drug Targeting

Publication details, including instructions for authors and subscription information:

<http://www.tandfonline.com/loi/idrt20>

Glucosamine anchored cancer targeted nano-vesicular drug delivery system of doxorubicin

Smita Pawar^a & Pradeep Vavia^a

^a Department of Pharmaceutical Sciences and Technology, Institute of Chemical Technology, Mumbai, India

Published online: 08 Jul 2015.

To cite this article: Smita Pawar & Pradeep Vavia (2015): Glucosamine anchored cancer targeted nano-vesicular drug delivery system of doxorubicin, Journal of Drug Targeting

To link to this article: <http://dx.doi.org/10.3109/1061186X.2015.1055572>

PLEASE SCROLL DOWN FOR ARTICLE

Taylor & Francis makes every effort to ensure the accuracy of all the information (the "Content") contained in the publications on our platform. However, Taylor & Francis, our agents, and our licensors make no representations or warranties whatsoever as to the accuracy, completeness, or suitability for any purpose of the Content. Any opinions and views expressed in this publication are the opinions and views of the authors, and are not the views of or endorsed by Taylor & Francis. The accuracy of the Content should not be relied upon and should be independently verified with primary sources of information. Taylor and Francis shall not be liable for any losses, actions, claims, proceedings, demands, costs, expenses, damages, and other liabilities whatsoever or howsoever caused arising directly or indirectly in connection with, in relation to or arising out of the use of the Content.

This article may be used for research, teaching, and private study purposes. Any substantial or systematic reproduction, redistribution, reselling, loan, sub-licensing, systematic supply, or distribution in any form to anyone is expressly forbidden. Terms & Conditions of access and use can be found at <http://www.tandfonline.com/page/terms-and-conditions>

ORIGINAL ARTICLE

Glucosamine anchored cancer targeted nano-vesicular drug delivery system of doxorubicin

Smita Pawar and Pradeep Vavia

Department of Pharmaceutical Sciences and Technology, Institute of Chemical Technology, Mumbai, India

Abstract

Background: Efficacy of an anticancer drug is challenged by severe adverse effects persuaded by the drug itself; hence designing a tumour targeted delivery system is chosen as an objective of this research work.

Purpose: We propose, glucose transporter targeting ligand, i.e. synthesised *N*-lauryl glucosamine (NLG) anchored doxorubicin (DOX) in niosomal formulation.

Methods: Synthesised NLG was incorporated into niosomal formulation of DOX using Span 60 as surfactant, cholesterol as membrane stabilizer and dicetyl phosphate (DCP) as stabilizer.

Results: The formulation was stable with particle size of 110 ± 5 nm, zeta potential -30 ± 5 mV and entrapment efficiency approximately 95%. DSC and XRD pattern of freeze-dried formulation demonstrated encapsulation of DOX in niosomal formulation. Cytotoxicity of targeted niosomal formulation ($IC_{50} = 0.830$ ppm) was higher than non-targeted niosomal formulation ($IC_{50} = 1.369$ ppm) against B6F10 melanoma cell lines. *In vitro* cellular internalization revealed that targeted niosomal formulation was internalised more efficiently with higher cellular retention by cancer cells compared to the non-targeted niosomal formulation and free DOX. *In vitro* receptor binding and docking study of targeted niosomal formulation had shown the comparative association potential with glucose receptor.

Conclusion: NLG anchored niosomal formulation of DOX with enhanced cytotoxicity, internalization and receptor binding potential has implication in targeted cancer therapy.

Keywords

Docking study, doxorubicin, glucose transporter proteins, niosomes, *N*-lauryl glucosamine

History

Received 25 March 2015
Revised 17 May 2015
Accepted 24 May 2015
Published online 7 July 2015

Introduction

Till date, chemotherapy is a commonly used approach for the treatment of cancer [1]. However, chemotherapy is having many limitations owing to poor physicochemical properties, such as hydrophobicity/hydrophilicity, short half-life, instability or the toxicity related to normal healthy tissues or organs [2]. Doxorubicin (DOX), an anthracycline antibiotic, has a broad spectrum anticancer potential against wide range of tumours [3]. However, effective delivery of DOX to tumour target is extremely a challenging task, because of short distribution half-life, resistance, intolerance, severe side effects and high systemic toxicity to normal healthy tissue cells, especially cardio-toxicity [4]. Therefore, targeted drug delivery systems have become a thrust area of researchers to overcome these challenges. Nanocarrier-based drug delivery system is a promising approach for targeted drug delivery to tumour tissue, since it offers sustained

release of drug over a longer period of time, reduces systemic toxicity, enhances targeting by a mechanism called “enhance permeation and retention” (EPR) effect, improves the pharmacokinetic and therapeutic performance of the drug [5–7]. Nanocarrier drug delivery system enhances drug targeting to tumour tissue by passive targeting mechanism. Nanocarriers accumulate easily to the leaky vasculature of tumour and achieve higher residence due to the absence of lymphatic drainage [8]. Furthermore, nanocarriers functionalized with targeting ligand can lead to preferential localization of anticancer agent into cancerous cells which ultimately improve the specificity, therapeutic index and reduce systemic toxicity [9,10]. There are various nanocarrier drug delivery systems studied to deliver anticancer agents, such as polymer conjugate [11], polymeric micelles [12], polymeric nanoparticles [13], nanosponges [14], niosomes [15] and liposomes [16]. Liposomes are most widely explored for anticancer formulation and are very well accepted approach; however, liposomes have some reservations, *viz* storage stability (mainly oxidation of phospholipid) and leakage of entrapped drugs. In addition to that, liposomes are made up of synthetic phospholipids which are usually expensive and on the other hand, natural phospholipid shows a variable degree of purity [17]. A promising alternative approach to replace liposome is the use

Address for correspondence: Prof. Pradeep R. Vavia, Department of Pharmaceutical Sciences and Technology, Center for Novel Drug Delivery Systems, Institute of Chemical Technology, University under Section 3 of UGC Act – 1956, Elite Status and Center of Excellence – Govt. of Maharashtra, TEQIP Phase II Funded, N. P. Marg, Matunga (E), Mumbai 400 019, India. Tel: +91 22 3361 2220. Fax: +91 22 2414 5614. E-mail: pr.vavia@ictmumbai.edu.in

of liposome-like vesicular system made up of non-ionic surfactants, “niosomes”. Niosomes have wide applications in topical, oral and systemic delivery. A number of *in vivo* protocols supported that non-ionic surfactant vesicles, niosomes behave like liposomes, by extending the circulation of encapsulated drugs, by improving organ drug distribution and its metabolic protection [18]. However, niosomes show some advantages over liposomes, for instance, low cost, significantly higher chemical stability (with respect to oxidation) and low drug leakage [19]. The specificity of niosome towards cancerous cells has to be enhanced to increase efficacy and reduce the systemic toxicity associated with anticancer agents. Many studies have been reported pertaining to the delivery of chemotherapeutic agents at the targeted sites exploring various ligands, such as sugars, fatty acids, peptides, monoclonal antibodies, folic acid and transferrin [20]. Cancer cells have different physiology compared to the normal cells. The cancerous cells are in hypoxic conditions due to the absence of blood supply to tumour tissue which leads to modification in metabolic pathways for instance, by inhibiting the oxygen-dependent process of mitochondrial oxidative phosphorylation (OXPHOS) [21]. Hypoxia cooperates for adenine triphosphate (ATP) generation, thus mainly relies on glycolysis as an energy source. Increase in glycolysis causes an instant availability of ATP at the cost of large quantities of glucose, leading to lactic acid production. This causes the significantly increase in demand of glucose in tumour cells as more than 200-times greater than that of normal cells, it is termed as “Warburg effect” [22]. As a result, the HIF-1 α /HIF-1 β complex activates the transcription of genes encoding glucose transporters (GLUTs) and glycolytic pathway enzymes. This leads to overexpression of GLUTs in tumour tissue including lung, breast, prostate, melanoma, gastric, etc. to facilitate the uptake of glucose across the phospholipid membrane and into the cell [23]. Thus, designing targeted drug delivery system exploring glucosamine, a glucose sugar as a targeting ligand is very innovative and promising approach. Earlier study was published based on designing of polymer drug conjugate system using glucosamine as targeting ligand and demonstrated promising results for anticancer activity [20]. Present work is focused on synthesis and evaluation of fatty acid derivative of glucosamine by *N*-hydroxy succinimide (NHS) activation of glucosamine and subsequently conjugation with fatty acid by EDC.HCL. Further, we have demonstrated design, development and *in vitro* evaluation of targeted niosomes of DOX anchoring fatty acid derivative of glucosamine as a targeting moiety for enhanced cellular delivery and anticancer activity. We have proposed targeted niosomal delivery of DOX consisting of non-ionic surfactant-based niosomes as a carrier, DOX as an anticancer drug and glucosamine as a targeting ligand/penetration enhancer. In addition, comparative cellular localization dynamics of DOX solution and targeted niosomal formulation of DOX were evaluated. *In vitro* cytotoxicity of the niosomal formulation was studied and compared using B6F10 skin melanoma cancer cells. Finally, glucose receptor targeting approach was justified with *in vitro* fluorescence study and *in silico* docking study of synthesised targeting ligand anchored niosomes of DOX.

Materials and methods

Materials

DOX was procured as a gift sample by RPG Life sciences, India. Span 60, Tween 80 and cholesterol were procured from S. D. Fine Chemicals, India. D-Glucosamine sulphate, dicycyl phosphate (DCP), *N*-(3-dimethylaminopropyl)-*N*-ethylcarbodiimide HCl (EDC.HCl) and *N,N*-diisopropyl-ethylamine, 4-(methylamino) pyridine (DMAP) were procured from SigmaAldrich, India. Concanavallin A was purchased from SRL, India. Dialysis membrane of molecular weight cut off 10–12 kDa was purchased from Hi-media, India. B6F10 skin melanoma was procured from ATCC. Sulforhodamine (SRB) was purchased from Invitrogen, India. All other chemicals and solvents were of analytical grade purchased from S. D. Fine Chemicals, India and used without purification.

Synthesis of *N*-lauryl-glucosamine (NLG)

NLG was synthesised by two steps process, such as first formation of NHS (*N*-hydroxy succinimide)-ester of lauric acid and then reaction of NHS activated lauric acid with glucosamine (NLG) [24].

NHS-ester of lauric acid

Briefly, NHS-activated lauric acid was synthesised by the addition of lauric acid (10 mM) into solution of NHS (12 mM) in dry ethyl acetate (40 ml). Dicyclohexylcarbodiimide (DCC) (15 mM) was then added to form highly unstable activated intermediate and the reaction mixture was left to incubate overnight at room temperature and reaction was monitored by thin layer chromatography (TLC) (chloroform:diethyl ether, 8:2). The precipitated form of dicyclohexylurea was separated by filtration and solvent was removed under reduced pressure to yield white crystalline powder. The product was further purified by repeated recrystallization from ethanol.

N-lauryl-glucosamine (NLG)

Glucosamine (10 mM) was dissolved into DMSO (30 ml) with triethylamine (0.1 ml). Lauric acid NHS ester (10 mM) dissolved in chloroform was added to the above solution. The reaction mixture was stirred for a 48-h period at room temperature. After this, chloroform was removed at reduced pressure. NLG was then precipitated with water and recovered on a sintered glass filter. The resulting powder was purified by washing repeatedly with water and chloroform. It was then dried at 40 °C. The reaction was monitored by TLC (butanol:acetic acid:water; 3:1:1). The purified sample was characterized for Fourier transform infrared spectroscopy (FTIR), mass, nuclear magnetic resonance (NMR), melting point, etc.

Preparation of niosomes

Different methods and surfactants were tried to formulate niosomal drug delivery system.

Thin film hydration

Niosomes were prepared from two different components, namely the non-ionic surfactants, such as SpanTM, TweenTM,

DCP and cholesterol. The mixture was placed in a 100 ml round bottom flask and dissolved in chloroform. The organic solvent (chloroform) was removed under vacuum using a rotary evaporator (Buchi Rotavapor R-114, Buchi, Switzerland) at a rotation speed of 150 rpm with the flask being partially immersed in a water bath previously adjusted to 40 °C. After 1 h, the rotary evaporator was switched off, the negative pressure was released and the flask was detached. A thin film of dry surfactant/cholesterol mixture was seen on the inner surfaces of the flask. The dry film was hydrated with DOX containing phosphate buffer saline (PBS, pH 7.4) (10 ml; 55–60 °C) followed by hand-shaking for 10 min. The niosomal suspension was left overnight to ensure complete hydration of surfactant molecules and proper formation of niosomes. The various surfactants were screened with respect to stability, entrapment efficiency and particle size of niosomes.

Ethanol injection

Briefly, weighed quantities of the surfactants (Span™, Tween™), cholesterol (in different molar ratios *viz.* 1:1, 1.5:1, 1:1.5, 2:1 and 1:2) and DCP were dissolved in ethanol at 45–50 °C. DOX was dissolved in PBS (pH 7.4). DOX solution was heated and maintained up to 60 °C by using a water bath. The above ethanolic solution was then added rapidly (5 ml/min) to the heated DOX solution with the help of needle (gauge size 26) and syringe with stirring (1000 rpm). As the ethanol gets evaporated, turbid red colored mixture was formed. The trace of ethanol was then removed under vacuum in a rotary evaporator at 50 °C. The whole preparation method was performed at 60 °C, which is higher than the gel–liquid transition temperature (T_c) of surfactants. The resulted niosomal suspension was left to mature overnight at 4 °C and stored at refrigerator temperature for further studies. Initially, different surfactants were identified and screened for their vesicle forming ability and afterwards, DOX-loaded niosomal formulation was optimized on the basis of the effect of cholesterol and DOX loading on niosomes size, stability and entrapment efficiency. The targeted niosomes using NLG (TAR DoxNio) was prepared using the protocol same as above, with the addition of NLG into ethanolic mixture of surfactant and cholesterol. The resulted dispersion was subjected to ultracentrifuge at 35 000 rpm at 20 °C for 1 h to get pellets of niosomes. The resulted niosomes were subjected to freeze drying using trehalose (1:10) as cryoprotectant.

Particle size and zeta potential

The average particle size, size distribution and zeta potential of niosomal formulation were measured using Zetasizer (Malvern Instruments, Malvern, Worcestershire, UK). Freshly prepared targeted and non-targeted DOX-niosomes were diluted with Milli-Q water, and freeze-dried niosomes were reconstituted in Milli-Q water with sonication. The stability and integrity of niosomal structure were studied by calculating the ratio of mean particle size (S_f) of niosomal formulation after reconstitution of freeze-dried samples and the initial mean particle size of niosomes (S_i) before freeze-drying.

Entrapment efficiency

For determination of DOX entrapment, niosomal suspension was ultra-centrifuged (Thermo Sorwall WX Ultra, Marietta, OH) at 35 000 rpm at 20 °C for 1 h. The supernatant was separated and settled pellets were washed with Milli Q water to completely remove the free DOX. The amount of entrapped DOX was determined by rupturing of the vesicles by treatment with isopropyl alcohol. The DOX content was determined by high-performance liquid chromatography (HPLC) using a Hypersil ODS-5 column with a mobile phase consisting of 0.05 mol/l potassium dihydrogen phosphate–acetonitrile (65:35, v/v) at a flow rate of 1.0 ml/min, and DOX was detected at λ_{\max} 230 nm. The percentage of drug entrapped was calculated from the ratio of the DOX in the vesicles to the total amount of DOX in the aqueous suspension.

Stability of DOX-niosomes

The niosomal DOX dispersion was subjected to stability study at 4 and 25 °C and particle size, zeta potential and entrapment efficiency were monitored. The DOX leakage, zeta potential and particle size were evaluated at 0 and 15 days.

Morphology of niosomes

The morphological examination of niosome was performed using environmental-scanning electron microscope (ESEM) (JEOL JSM-840 SEM HITACHI, Japan). Very dilute suspension of niosome vesicles in distilled water was mounted on adhesive carbon tape and dried at room temperature; they were coated with platinum under vacuum and examined on microscope.

XRD and DSC

The freeze-dried non-targeted DOX-loaded niosomes (NTAR NioDOX) and NLG anchored TAR NioDOX were subjected to X-ray diffractometer (XRD) and differential scanning calorimetry (DSC) analysis for evaluation of encapsulation of DOX into vesicular core of niosomes. DSC for pure drug and niosomal lyophilized samples was performed with Pyris 6 DSC (Perkin Elmer, Waltham, MA) instrument under a pure nitrogen flux with a heating rate of 10 °C/min in the temperature range from 40 to 250 °C. Each sample was accurately weighted (1–2 mg) in an aluminium pan and then crimped and sealed. Blank aluminium pan was used as reference for analysis. XRD analysis, analytical X-ray diffractometer (Model - Xpert PRO MPD, Make: Panalytical, Netherland) with a Cu K α line as a source of radiation was used. The conditions used for analysis were 40 kV voltage, 30 mA current and a scanning rate of 0.02°/min over a 2θ range of 2°–40°.

***In vitro* drug release**

In vitro release studies of targeted and non-targeted niosomes loaded with DOX were performed using a dialysis membrane (dialysis cellulose membrane, molecular-weight cut-off 10–12 KDa, Merck Millipore, India) [25]. The dialysis membrane was pre-treated with PBS (pH 7.4) for 1 h to ensure its wetting and sealing. Drug-loaded niosomal

suspensions (2 ml) in PBS pH 7.4 were placed in dialysis tube. This latter was immersed into 50 ml of PBS (pH 7.4) release medium at 100 rpm and temperature 37 °C. At predetermined time intervals, aliquot samples of release medium were withdrawn and replaced with equal volume of fresh release medium. The drug concentrations in the release medium were measured by using HPLC analysis, as described above in section “Entrapment efficiency” under “Materials and methods”.

In vitro hemolysis study

In vitro hemolysis is the most important and preferable method for the assessment of parenteral safety of formulation [26]. Freshly collected human blood was centrifuged to separate RBCs. The separated RBCs were washed thrice with PBS. Various concentrations of DOX from DOX solution, NTAR NioDOX and TAR NioDOX in the range of 5–200 µg/ml were mixed with 200 µl of RBCs solution and the final mixture volume was made upto 1 ml with PBS. The deionized water and PBS were used as positive and negative control, respectively. The reaction mixture was kept at 37 °C for 1 h. After completion of the reaction, mixture was centrifuged at 5000 rpm for 5 min and supernatant was analysed at 540 nm. PBS was used as the negative control and the detergent, sodium lauryl sulfate (SLS) was used as positive control (100% hemoglobin release). The % hemolysis was calculated from Equation (1)

$$\% \text{Haemolysis} = \frac{\left(\begin{array}{l} \text{absorbance of test samples} \\ - \text{absorbance of negative control} \end{array} \right)}{\left(\begin{array}{l} \text{absorbance of positive control} \\ - \text{absorbance of negative control} \end{array} \right)} \times 100 \quad (1)$$

In vitro cell line study

B6F10 cell lines were cultured in 96-well plate (cell count: 2×10^5 cells/ml) using DEME culture medium with 10% foetal bovine serum. These cells were incubated in culture medium with increasing concentrations of DOX, NTAR NioDOX and TAR NioDOX. After 48 h of growth, cells were fixed by 100 µl of cold 10% w/v trichloroacetic acid and kept it for 4 h at 4 °C. The 96-well plate was washed three to four times with distilled water and excess water was wiped with tissue paper. Furthermore, 96-well plate was air dried at room temperature. A 100 µl of 0.057% w/v SRB solution was injected to each well and incubated at room temperature for 30 min and subsequently 96-well plate was rinsed off with 1% v/v acetic acid solution four times to remove unbound dye. Afterwards, 200 µl of 10 mM Trisbases (pH 10.5) was added to each well and incubate on shaker for 5 min to solubilised protein bound dye and the absorbance was measured at λ_{max} of 510 nm on an ELISA plate reader [27].

In vitro receptor binding by fluorescence

The underlining principle of the present study is fluorescence quenching of lectin [concanavallin A (CON A)] upon association with carbohydrates. CON A has maximum absorption at 280 nm and fluorescence emission wavelength

at 332 nm [28]. According to earlier studies, the fluorescence analysis was considered as the potential, sensitive and accurate technique to study molecular interaction including protein and carbohydrate association [29]. The study was focused to derive association and dissociation potential of NLG and NLG anchored NioDOX with CON A. Stock solution of CON A (1 µg/ml) in PBS (pH 7.4) was prepared. The study was conducted at human body temperature, i.e. 37 °C. The fluorescence spectra of CON A was recorded with absorption at 280 nm and emission at 300–500 nm using fluorescence spectrophotometer at slit width of 2.5 and 5. Furthermore, the increasing concentration of NLG and NLG anchored NioDOX was added into CON A solution and the corresponding fluorescence spectrum was recorded. The resultant data were further processed by Chipman method [30] and binding as well as dissociation constant was derived. The plot of $\log[C]f$ versus $\log\{(\Delta F)/(F_c - F_\infty)\}$ offered K_a value as abscissa intercept and slope as number of binding site for lectin–analyte interaction according to Equation (2), where $[C]f$ is the free analyte concentration. The dissociation constant was calculated as inverse of K_a value

$$\log[(F_0 - F_c)/(F_c - F_\infty)] = \log K_a + \log \left\{ [C]t - [P]t \left(\frac{\Delta F}{F_\infty} \right) \right\} \quad (2)$$

In silico docking study

It is very important to understand the *in vivo* binding potential of ligands to specific receptors. To analyse the receptor binding potential, molecular flexible docking studies were performed by the grid-based ligand docking with energies (Glide) [31–33]. The computational program was run within Maestro [33] and a graphical user interface by Schrödinger, LLC, New York, NY. CON A, representative of glucose transporter receptor, is a homotetramer. The 3D structure of CON A for carbohydrate recognition domain was downloaded from Protein Data Bank (PDB code 5CN A, 10 of resolution) (<http://www.rcsb.org/pdb/explore/jmol.do?structureId=5CNA&bionumber=1>). Before performing docking analysis of ligands, structural defects within imported protein structure were corrected and generated by protein preparation wizard using Maestro. All crystallographic water molecules, other than the molecules forming coordinate bonds were removed. Further, protein structure was relieved from any strain and was fine-tuned using OPLS 2005 force field. The respective ligands including *N*-acetyl glucosamine and NLG structures were constructed using the 2D Sketcher in Maestro. 3D conformation of ligand with minimum energy was generated with the help of LigPrep [34], using OPLS 2005 force field. The grid, i.e. a virtual box having a default length of 10 Å, was generated to limit the docking process to handle within the grid space.

In vitro cellular internalization

B6F10 skin melanoma cancer cells were seeded in 96-well plates at a density of 2×10^5 cells per well and incubated overnight at 37 °C. After attaining to confluence by cell, cell monolayers were washed with DEME media and incubated

with test samples as DOX, NTAR NioDOX and TAR NioDOX. All test samples were diluted with DEME media and adjusted to 10 ppm DOX or DOX equivalent concentration. Cells were treated with test samples at 37 °C for 0.5, 1 and 2 h. Cells were washed twice with ice-cold PBS (pH 7.4) and lysed with PBS containing 0.5% sodium lauryl sulphate at 37 °C for 30 min. DOX concentrations in cell lysates were measured by HPLC as described above in section ‘‘Entrapment efficiency’’ under ‘‘Materials and methods’’.

Result and discussion

Synthesis of *N*-lauryl glucosamine

The synthesis of NLG is schematically represented in Figure 1.

¹HNMR

¹HNMR spectra of *N*-hydroxy succinimide of lauric acid and NLG were recorded on 500 MHz spectrophotometer using CDCl₃ and DMSO-d₆ solvent, respectively. A typical ¹HNMR spectrum of *N*-hydroxy succinimide of lauric acid and NLG is shown in Figure 2(A) and (B). The peaks at δ 0.91 (3H, s, CH₃, lauryl), 1.29 (CH₃–CH₂, lauryl), 2.18 (CH₂–C00) 2.85 (–CH, NHS) have indicated the formation of NHS ester of lauric acid (Figure 2A). Figure 2(B) confirms the formation of NLG, as retention of lauric acid characteristic peak and additional peak of sugar (3–4.5) and amide hydrogen (6.14).

FTIR

A comparative FTIR spectrum of lauric acid, NHS ester of lauric acid and NLG is represented in Figure 3. Lauric acid has characteristic carbonyl C–O stretch at 1700 cm⁻¹. However, in case of NHS ester of lauric acid, the amide C–O stretch is observed at 1648 cm⁻¹ and in case of NLG, the ester C–O stretch is observed at 1750 cm⁻¹. Thus, all the characteristic peaks are supporting the synthesis of NLG.

Mass spectroscopy and melting point

The mass of lauric acid is reported as 200 and melting point as 43 °C. Mass spectrometry data of NHS ester of lauric acid show a sharp peak at 285.29 (M⁺–OH) and NLG reveals one main peak corresponding to the mass ion 362 (100%, M⁺) and further minor peaks of (M⁺–OH) and 388 (M⁺+OH)

(Figure 4). These results indicate that NLG was successfully synthesised. From the DSC thermogram, the melting point of the synthesised NHS ester and NLG was observed to be 75 and 198 °C, respectively (Figure 5).

DOX-niosomes

Niosomes were prepared by thin film hydration method and ethanol injection method. However, ethanol injection has given higher drug entrapment with minimum particle size as compared to thin film hydration method (data not given). DOX niosomes and NLG anchored DOX-niosomes were formulated using Span 60 as surfactant, cholesterol as bilayer membrane stabilizer and DCP as charge stabilizer. Span 60 has given highest drug entrapment than Tween 80. The highest drug entrapment achieved using Span 60 may be due to solid property, low hydrophilic-lipophilic balance (HLB) (4.7), i.e. high hydrophobicity and high phase transition temperature [35]. Thus, hydrophobic portion of DOX may have high affinity for hydrophobic core of Span 60. The optimized formula and processing conditions for the niosomes are given in Table 1. The optimized formulation was stable in liquid dispersion and solid freeze-dried form with respect to particle size, drug content and entrapment.

Particle size and zeta potential

An ideal nano-carrier system for targeting cancer tumour cell should possess particle size below 200 nm to avoid reticulo-endothelial system and passively target cancerous tissue through EPR effect [36]. Particle size of optimized formulation was observed to be 110 ± 5 nm with poly dispersability index (PDI) 0.256. Developed formulation was further diluted with PBS (pH 7.4) as 1:100 and particle size was measured as 105 ± 4 nm with PDI 0.202. Hence, it justifies a non-significant impact of dilution on particle size, suggesting the stability of the developed formulation. Freeze-dried sample (5% w/w trehalose) has shown particle size around 130 ± 4 nm with PDI 0.265. Thus, ratio of particle size (S_f) of niosomal formulation after reconstitution of freeze-dried samples and initial particle size of niosomes (S_i) before freeze-drying was found to be 1.20. The value near to 1 suggests the good redispersion capacity.

Zeta potential is another important index for the stability of a colloid system, such as niosomal formulation. Higher value of zeta potential indicates high electric charge on the surface of drug-loaded niosomes, which will result in strong repulsive

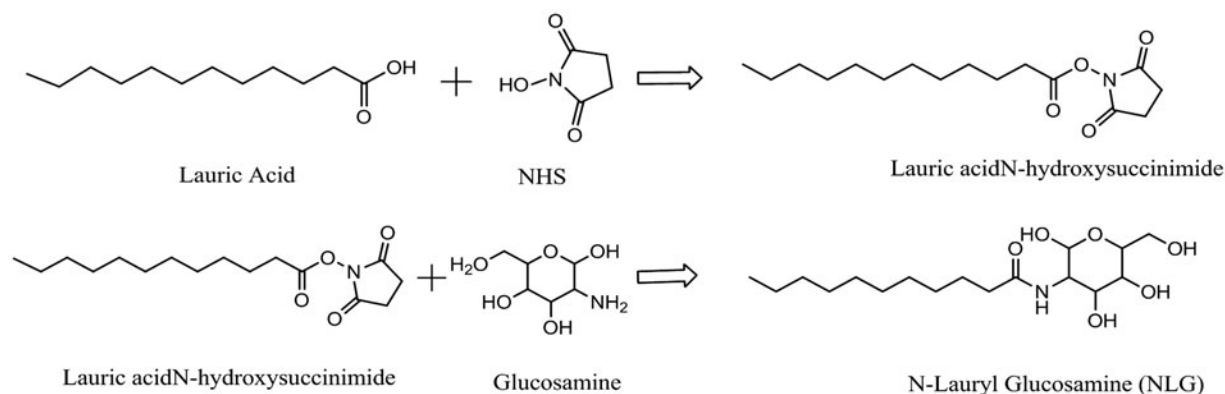


Figure 1. Synthesis scheme of *N*-lauryl glucosamine.

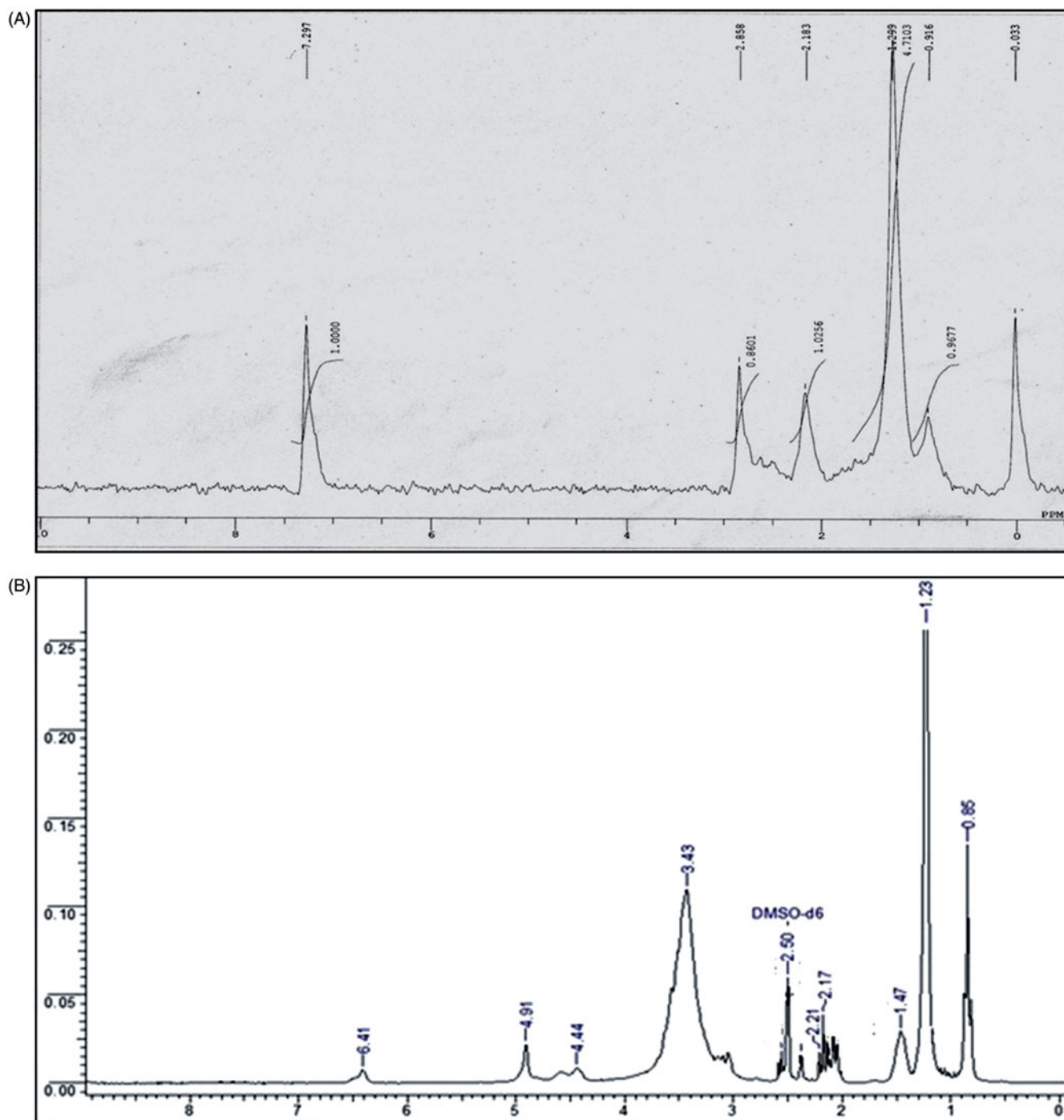


Figure 2. ¹H NMR of NHS-ester of lauric acid (A) and NLG (B) by using CDCl₃ and DMSO, respectively.

forces among the particles to prevent aggregation and setting of nanoparticles, eventually contributing to the stability of nano-dispersion. Zeta potential of the blank and drug-loaded niosomal formulation was observed to be -40 ± 5 and -30 ± 3 mV, respectively. Negative zeta potential of niosomes may be due to the presence of terminal phosphate groups of DCP [35].

Entrapment efficiency

Due to unique closed bilayer structure and physicochemical properties of niosomes, different types of functional components can be encapsulated into the interior of niosomes or

incorporated into the surfactant bilayer membrane or adhered to the vesicles [37]. Entrapment efficiency, a prime important parameter in niosome drug delivery system, is closely related to the niosome preparation method and formulation. The entrapment of DOX-niosomes was found to be nearly 90% as quantified by HPLC analysis. The entrapment efficiency increased as concentration of Span 60 was increased and decreased as concentration of DOX was increased. Increasing concentration of Span 60 resulted in more space to hold and entrap DOX. On the other hand, as the concentration of DOX increases, due to less space in vesicular core or bilayer region resulted in less entrapment of DOX. Thus, optimized drug loading was 15% with respect to surfactant load.

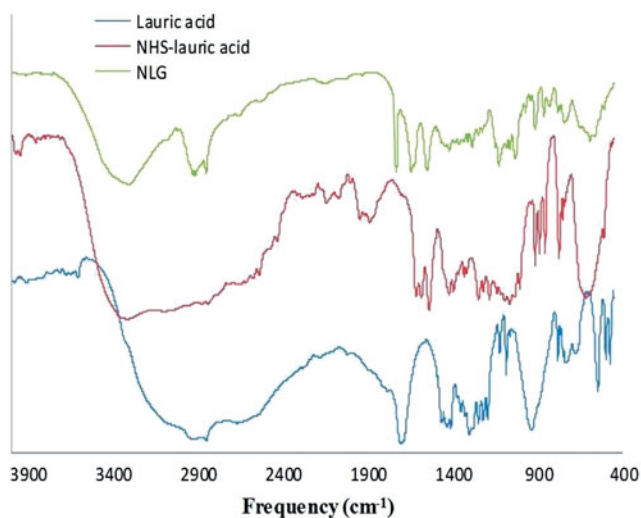


Figure 3. FTIR of lauric acid, NHS-ester of lauric acid and NLG.

Figure 4. Mass spectra of NHS-ester of lauric acid (A) and *N*-lauryl glucosamine (NLG) (B) by electrospray ionization-mass spectroscopy (ESI-MS).

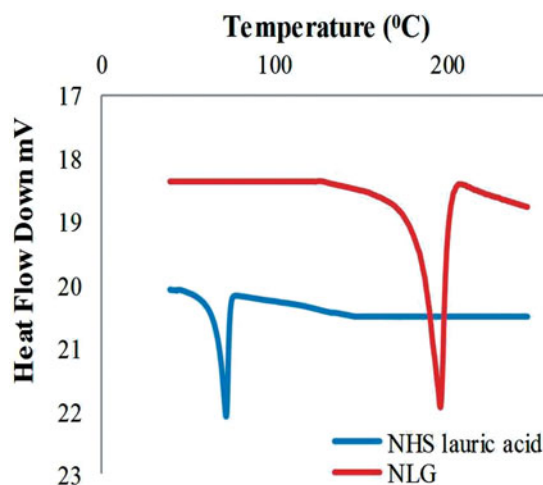
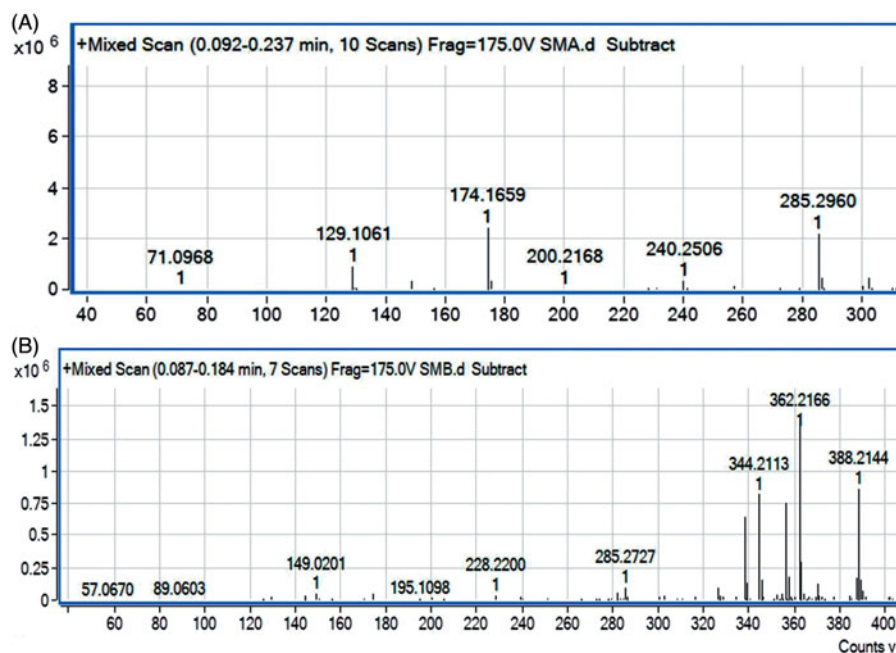


Figure 5. DSC thermogram of NHS-ester of lauric acid and *N*-lauryl glucosamine (NLG) is showing melting point around 75 and 198°C, respectively.

Stability

The stability of niosomal dispersion is of vital importance from efficacy preview. The formulation was observed to be stable with minimal variation in particle size, zeta potential and entrapment of niosomal DOX formulation in comparison with initial formulation at two different temperature conditions (Table 2). Higher zeta potential and low particle size of DOX niosomes had resulted good stability.

Morphology of niosomes

The environmental SEM micrograph of DOX-niosomes is shown in Figure 6. Micrograph reveals that nanoparticles were found to be spherical in nature with particle size below 200 nm and no aggregation of particles. Electrostatic repulsion force between the negatively charged DCP chains on the

surface of niosomes could be probably the reason for stable structural morphology of niosomes. The particle size as estimated by the ESEM was in good agreement with that determined by the Zetasizer. In previous section ‘‘Particle size and zeta potential’’, the observed particle size was below 200 nm.

DSC and XRD analysis of niosomes

Figure 7(A) shows DSC thermogram of DOX niosomes along with individual component. The DOX-niosomes and NLG anchored DOX-niosomes have shown absence of sharp endothermic peak of DOX at 220°C temperature. DSC thermogram had shown uniform entrapment of DOX into the vesicles of niosomes. These results were further confirmed by XRD analysis. Figure 7(B) shows XRD pattern of blank niosomes, DOX, NTAR NioDOX and TAR NioDOX.

However, XRD patterns of freeze-dried niosomes have not shown a sharp peak, indicating encapsulation of DOX. Thus, XRD pattern confirms a uniform entrapment of DOX into the vesicular core of niosomes.

In vitro drug release

In vitro drug release study was performed in phosphate buffer solution (pH 7.4) at 37°C. The cumulative percentage of DOX released from DOX solution, DOX-niosomes and NLG anchored DOX-niosomes as a function of time is shown in Figure 8. Figure 8 confirms slow and sustained release of DOX-niosomes. Besides, the drug release rate from NLG anchored DOX-niosomes are slightly higher than DOX-niosomes, which can be attributed to the hydrophilic nature of glucosamine and this distinct feature would help in long circulation of drug-loaded niosomes [38].

In vitro hemolysis study

In vitro hemolysis assay gives a quantitative indication of the damage caused by nanoparticles to red blood cells. The hemolytic ability of free DOX and DOX-loaded niosomes is shown in Figure 9. The result signifies the hemocompatibility of niosomes for parenteral drug delivery applications. Moreover, niosomal system had shown less than 15% of lysis in the whole experimental concentration range of DOX (5–200 µg/ml). Hemolytic potential of DOX diminished due to encapsulation of DOX into niosomal vesicle core and subsequently, the absence of direct contact of DOX with red blood cells. Thus, the results suggested that developed niosomal formulation of DOX possesses wide safety margin for parenteral administration.

In vitro cytotoxicity

The cytotoxic effects of DOX-loaded niosomes and free DOX on B6F10 skin melanoma cancer cells were evaluated using

the SRB assay (Figure 10). IC₅₀ value of niosomal formulation of DOX and free DOX is given in Table 3. Targeted and non-targeted niosomes without drug did not show any significant cytotoxic effect on the B6F10 skin melanoma cancer cells. Cell viability remained above 95%, confirming the non-toxic and biocompatible nature of niosomes. Drug-loaded TAR NioDOX and free DOX have exerted a similar cytotoxic effect but it is clearly superior to NTAR NioDOX. As free DOX enters into the cells by simple diffusion mechanism, while niosomal DOX enters through endocytosis and showed sustained released of DOX from niosomes, resulting in a reduced cytotoxicity. However, since TAR NioDOX has glucosamine as a targeting ligand, glucosamine would increase cellular uptake of this nanocarrier through glucose transporter protein which specifically binds to glucose sugars [39,40]. In addition to that, hydrophilic nature of glucosamine may have contributed to improve cellular internalization [38] and subsequently, similar cytotoxicity profile as free DOX.

In vitro receptor binding assay

In vitro cytotoxicity study had justified targeting potential of developed TARNio formulation of DOX. In addition to that, it is very essential to support finding with receptor interaction of glucosamine anchored niosomes with CON A, lectin having specific binding potential with glucose sugar like glucosamine [41]. CON A has auto fluorescence at excitation wavelength of 280 nm with emission wavelength of 320 nm. It was observed that incubation of glucosamine anchored

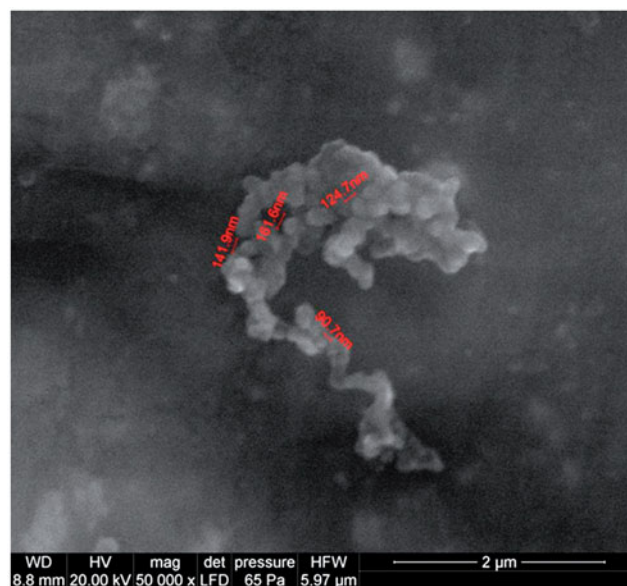


Figure 6. Environmental SEM micrograph of DOX-loaded niosomes.

Table 1. Optimized formulation and processing conditions for the preparation of niosomal formulation by ethanol injection method.

Formulation ingredients	NTAR	TAR	Processing conditions
	NioDOX (mg)	NioDOX (mg)	
Span 60	106	106	
Cholesterol	85	85	Temp.: 60–65 °C
Dicetyl phosphate	8	8	RPM: 500 rpm
DOX	15	15	Addition rate:
NLG	–	10	5 ml/min
Ethanol	3 ml	3 ml	Needle size: 26 guage
PBS buffer pH 7.4	10 ml	10 ml	
Trehalose	20	20	

Table 2. Stability studies of niosomal dispersion at 4 and 25 °C with respect to particle size, zeta potential and entrapment efficiency for period of 15 days.

Formulation	Particle size (nm)			Zeta potential (mV)			Entrapment efficiency (%)		
	Initial	4 °C	25 °C	Initial	4 °C	25 °C	Initial	4 °C	25 °C
NTAR NioDOX	105	108	112	–30	–28	–34	96	92	90
TAR NioDOX	110	115	120	–28	–31	–26	94	92	91

Figure 7. DSC thermogram (A) and XRD pattern (B) of freeze dried niosomal formulations of DOX in comparison with DOX.

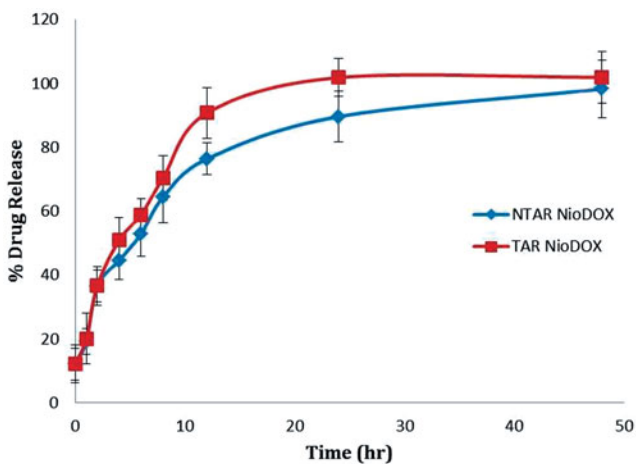
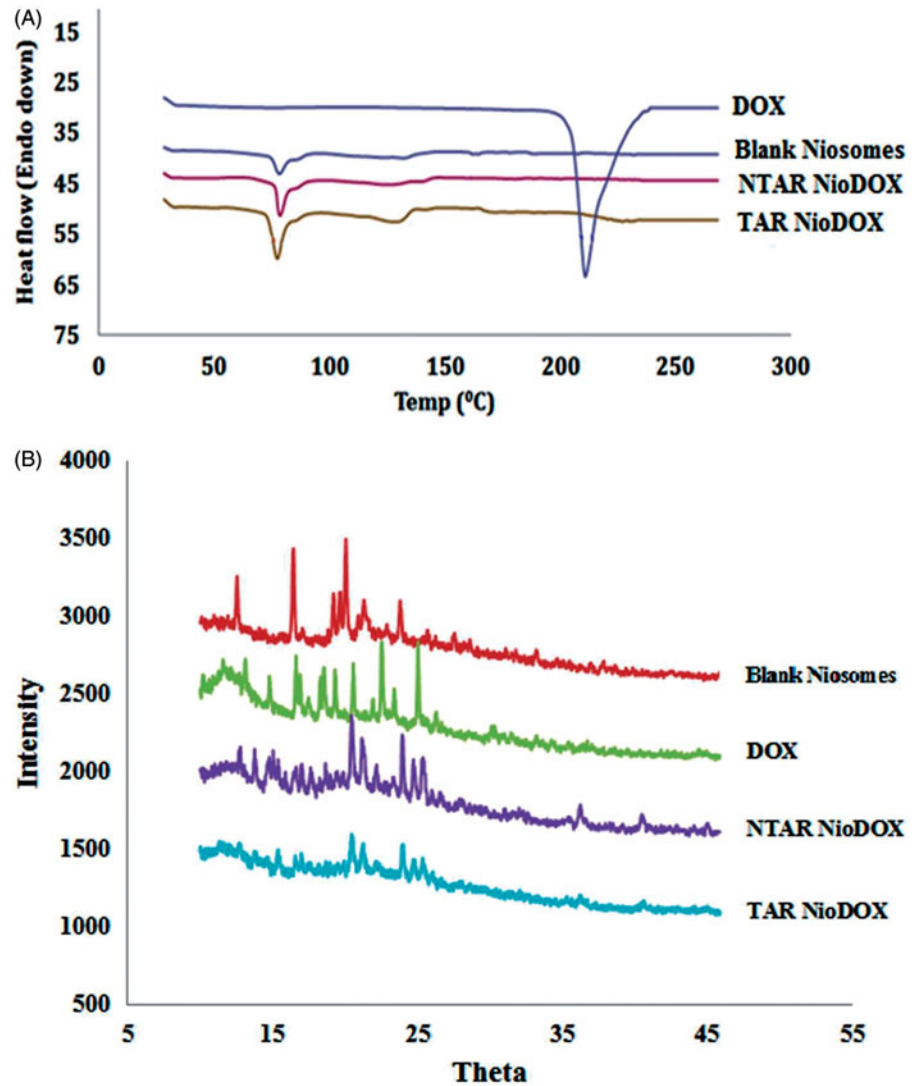


Figure 8. *In vitro* release profile of NTAR NioDOX and TAR NioDOX in pH 7.4 PBS buffer.

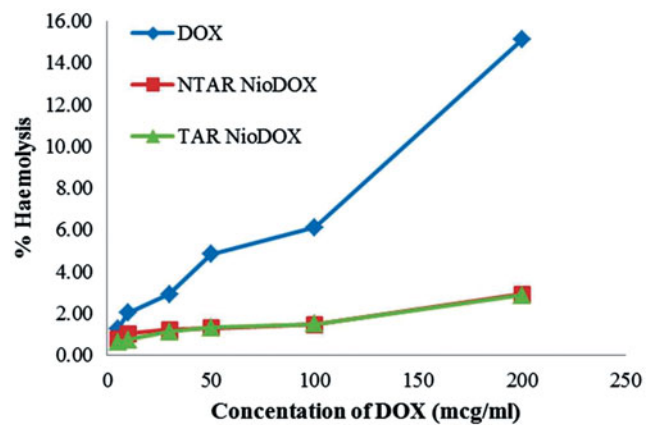


Figure 9. *In vitro* % hemolysis of DOX, NTAR NioDOX and TAR NioDOX on RBCs.

niosomal formulation with CON A resulted in quenching of fluorescence. The resulted quenching of fluorescence was further subjected to chipman equation to calculate binding constant of glucosamine with lectin. The binding constant, dissociation constant and number of binding sites are given

in Table 4. The result had implicated the promising interaction potential of glucosamine anchored niosomes with CON A. The binding constant and number of binding sites are found to be comparable to free glucosamine. Hence, the study indicates that the synthesised conjugate has retained

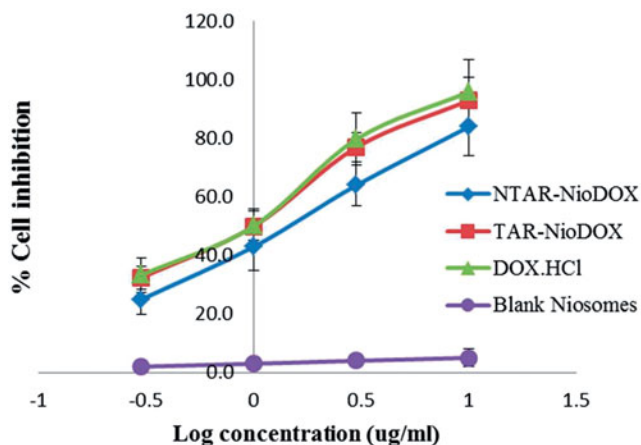


Figure 10. *In vitro* cytotoxicity of DOX, NTAR NioDOX and TAR NioDOX against B6F10 skin melanoma cell line by SRB assay.

Table 3. Cytotoxicity of free DOX drug, NTAR NioDOX and TAR NioDOX B6F10 skin melanoma cell line *in vitro*.

Formulation	IC ₅₀ (μM) of DOX equivalent
DOX. HCl solution	0.785*
NTAR NioDOX	1.369*
TAR NioDOX	0.830

**p* < 0.005 using ANOVA.

Table 4. *In vitro* receptor binding potential and number of binding sites of NLG and NLG anchored niosomes as TAR NioDOX using CON A, lectin as model receptor protein.

Parameters	N-Acetyl Glucosamine		
	NLG	TAR NioDOX	
Association constant (K_a) (M)	3.36×10^4	3.20×10^4	3.12×10^4
Dissociation constant (K_d) (M^{-1})	2.94×10^{-5}	3.12×10^{-5}	3.20×10^{-5}
Number of binding sites (N)	3.68	3.22	3.17

binding association potential with glucose receptors and can be endocytosed through receptor–ligand interaction.

In vitro cellular uptake

Figure 11 illustrates uptake profiles of DOX by B6F10 skin tumour cells treated with DOX and DOX formulations, all containing 10 ppm (17.2 μM) DOX at 0.5, 1 and 2 h time interval. After 2 h, the cellular level of DOX in tumour cell has reached maximum in case of TAR niosome as compare to NTAR niosome and free DOX. In case of DOX solution, initially uptake of DOX was very rapid and reached at higher concentration within 0.5 h, but uptake was reduced during next 2 h. However, targeted niosomal formulation has shown higher uptake with respect to time than non-targeted niosomes. Outflow of DOX from cells would be mediated by Pgp or other proteins, which are responsible for nuclear-cytoplasmic trafficking and compartmentalization of drugs [42]. However, in case of niosomal formulation, higher concentration into cells may be due to availability of different

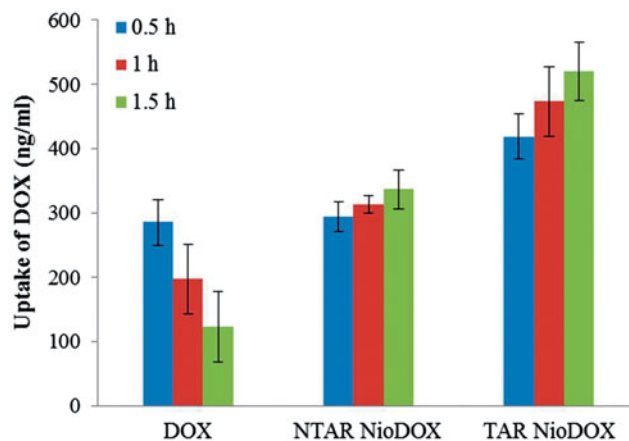


Figure 11. *In vitro* cellular uptake of DOX, NTAR NioDOX and TAR NioDOX against B6F10 skin melanoma cell line at 0.5, 1 and 2 h.

form of DOX. It is reported that higher concentration of DOX resulted in aggregation or molecular stacking and formation of dimeric form of DOX [43–45]. This phenomenon would explain lack of a cytotoxic advantage for glucosamine-targeted niosomal DOX over free DOX regardless of higher drug accumulation into the cells. It ultimately leads to the unavailability of DOX to be as a substrate for p-gp efflux. Above finding signifies that glucosamine anchored niosomes are showing receptor mediated internalization of niosomes *via* glucose transporter proteins which further enhances the cellular internalization of DOX than non-targeted niosomes [46–48].

In silico docking study

Docking analysis offers a complete understanding of ligand receptor binding based on physicochemical parameters. The active binding site for Con A could be easily located on the surface of the H1 subunit. Figure 12 shows optimized docked position of D-mannose at the active binding site and the interaction illustration of D-mannose with ConA. Following docking into the active site, the ligands were studied on the basis of their Glide score (or *G* score) and E_{model} scores [48]. The Glide score is defined as an experimental measuring function that analyses the ligand binding free energy. It is the collective measure of electrostatic and van der Waals interactions [49]. Model energy score (E_{model}) is sum of the energy grid score, the binding affinity and the internal strain energy (in flexible docking) of the model. Therefore, the E_{model} is a major function in selecting best-docked position for each ligand, which is then studied according to their Glide score. The Glide score and E_{model} scores of NAG and NLG are demonstrated in Table 5. The NLG and NAG ligands showed approximately similar score compared to the known ligand D-mannose and formed similar type of interactions with the active sites. All the ligands maintained the hydrophobic interaction of TYR 100 and ALA 207 with either of C3, C4, C5 or C6 atoms of monomer and are shown in Figure 12. D-mannose demonstrated six hydrogen bonds. Similarly, NAG and NLG also exhibited five hydrogen bonds, comparable to D-mannose. Docking study exhibited

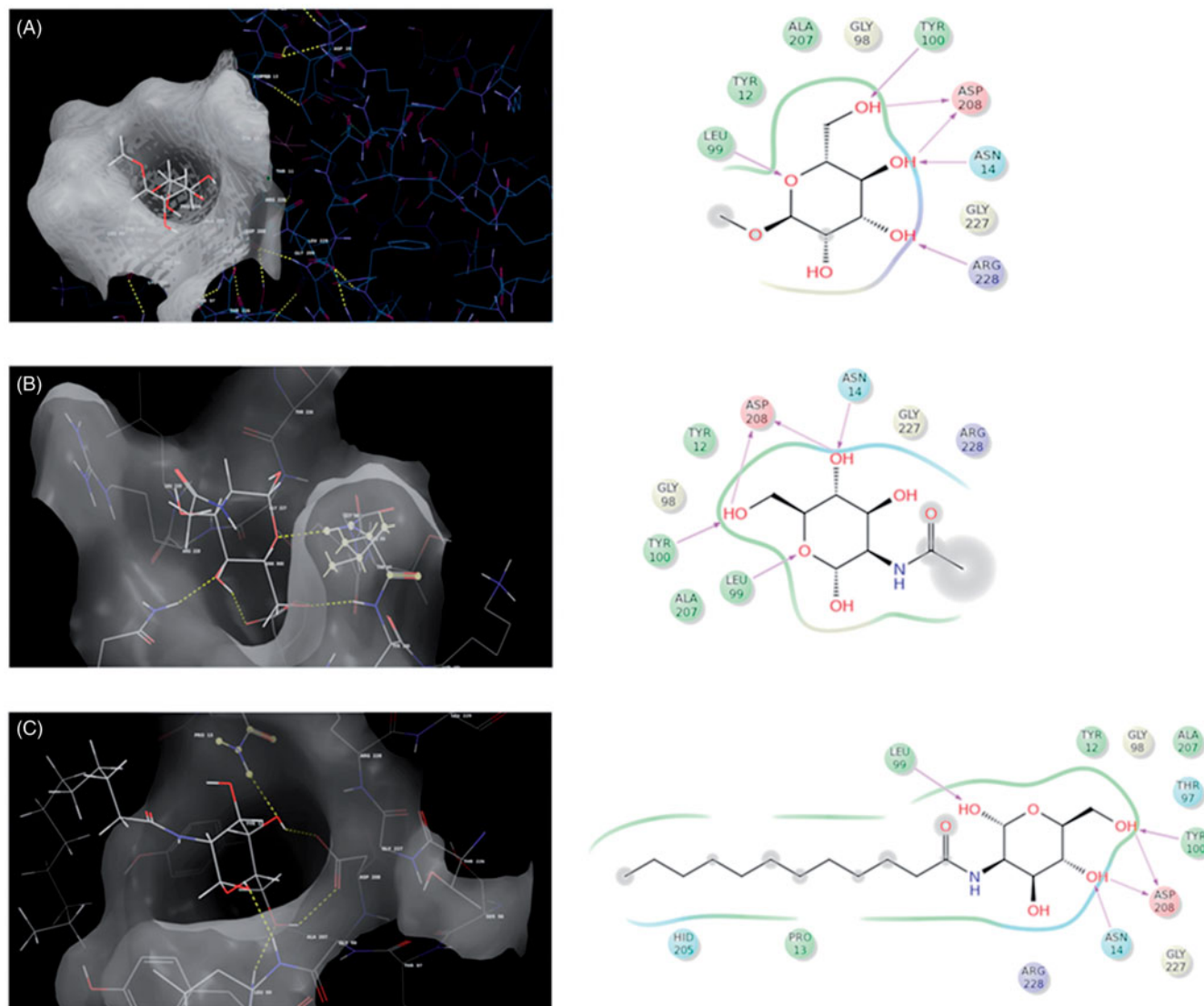


Figure 12. Docking analysis of standard (D-mannose), *N*-acetyl glucosamine and NLG with CON A.

Table 5. Docking results of various ligands in the original Con A crystal structure using Glide-XP.

Component	Glide score (kCal/mol)	E_{model} (kCal/mol)
Mannose (validation)	-6.599813	-52.073
<i>N</i> -acetyl glucosamine (NAG)	-5.309765	-42.9791
<i>N</i> -lauryl glucosamine (NLG)	-4.581725	-41.948

the significant binding affinity of NAG and NLG towards Con A. Thus, with comparable glide score, E_{model} scores, hydrogen binding and hydrophobic interaction of NLG, a synthesised targeting ligand proves the high possibility to target the glucose transporter receptors. Docking could definitely help in the preliminary screening of ligands for glucose receptor targeting.

Conclusion

Fatty acid derivative of glucosamine anchored niosomal formulation of DOX is formulated with high

entrapment efficiency and stability. *In vitro* cytotoxicity demonstrated higher cytotoxicity by targeted niosomal formulation compared to free DOX and non-targeted formulation. Cellular internalization study supports higher cellular internalization and retention of targeted niosomal formulation. In addition to that, accessibility of this targeting ligand to glucose specific lectin Con A is also presented by fluorescence spectroscopy and docking study. Offshoots of our findings offers an attractive and promising approach for delivering DOX into tumour cells, which is insensitive to Pgp-mediated drug efflux and more effective than free DOX and non-targeted niosomal DOX. Hence, the designed glucosylated targeted niosomal drug delivery can serve as promising approach for anticancer therapy.

Declaration of interest

The authors would like to thank UGC for providing financial assistance during the research work. The authors thank AICTE/NAFETIC for providing the facility to conduct research. Authors would like to thank RPG Lifesciences, India for providing doxorubicin.

References

- Gottesman MM, Fojo T, Bates SE. Multidrug resistance in cancer: role of ATP-dependent transporters. *Nat Rev Cancer* 2002;2:48–58.
- Si-Shen F, Shu C. Chemotherapeutic engineering: application and further development of chemical engineering principles for chemotherapy of cancer and other diseases. *Chem Eng Sci* 2003;58:4087–114.
- Pereverzeva E, Treschalin I, Bodyagin D, et al. Influence of the formulation on the tolerance profile of nanoparticle-bound doxorubicin in healthy rats: focus on cardio- and testicular toxicity. *Int J Pharm* 2007;337:346–56.
- Aarif YK, Peter PL, Thomas F, et al. Cardiotoxicity due to cancer therapy. *Cancer Heart* 2011;38:253–9.
- Moorthi CR, Manavalan K, Kathiresan K. Nanotherapeutics to overcome conventional cancer chemotherapy limitations. *J Pharm Pharmaceut Sci* 2011;14:67–77.
- Davis ME, Chen ZG, Shin DM. Nanoparticle therapeutics: an emerging treatment modality for cancer. *Nat Rev Drug Discov* 2008;7:771–82.
- Yogeshkumar M, Marilena L, Alexander MS. Liposomes and nanoparticles: nanosized vehicles for drug delivery in cancer. *Trends Pharmacol Sci* 2009;30:592–9.
- Xiao D, Russell JM. Nanomedicinal strategies to treat multi-drug-resistant tumors: current progress. *Nanomedicine (Lond)* 2010;5:597–615.
- Frank G, Rohit K, Andrew W, et al. Targeted nanoparticles for cancer therapy. *Nano Today* 2007;2:14–21.
- Lara SJ, Lilian EV, Sunita Y, Mansoor MA. Multi-functional nanocarriers to overcome tumor drug resistance. *Cancer Treat Rev* 2008;34:592–602.
- Ruth D. Polymer conjugates as anticancer nanomedicines. *Nat Rev Cancer* 2006;6:688–701.
- Chris O, Wouter B, Mariska B, et al. Polymeric micelles in anticancer therapy: targeting, imaging and triggered release. *Pharm Res* 2010;27:2569–89.
- Lilian EV, Mansoor MA. Multi-functional polymeric nanoparticles for tumour-targeted drug delivery. *Expert Opin Drug Deliv* 2006;3:205–16.
- Darandale SS, Vavia PR. Cyclodextrin-based nanosponges of curcumin: formulation and physicochemical characterization. *J Incl Phenom Macrocycl Chem* 2013;75:315–22.
- Uchegbu IF, Double JA, Kelland LR, et al. The activity of doxorubicin niosomes against an ovarian cancer cell line and three in vivo mouse tumour models. *J Drug Target* 1996;3:399–409.
- John WP. Liposome-based drug delivery in breast cancer treatment. *Breast Cancer Res* 2002;4:95–9.
- Carlotta M, Donatella P, Christian C, et al. Non-ionic surfactant vesicles in pulmonary glucocorticoid delivery: characterization and interaction with human lung fibroblasts. *J Control Release* 2010;147:127–35.
- Marzio LD, Marianecchi C, Cinque B, et al. pH-sensitive non-phospholipid vesicle and macrophage-like cells: binding, uptake and endocytotic pathway. *Biochim Biophys Acta* 2008;1778:2749–56.
- Jain CP, Vyas SP. Preparation and characterization of niosomes containing rifampicin for lung targeting. *J Microencapsul* 1995;12:401–7.
- Pawar SK, Badhwar AJ, Kharas F, et al. Design, synthesis and evaluation of N-acetyl glucosamine (NAG)-PEG-doxorubicin targeted conjugates for anticancer delivery. *Int J Pharm* 2012;436:183–93.
- Johanna C, Christiane BH, Jacques P. Tumour hypoxia induces a metabolic shift causing acidosis: a common feature in cancer. *J Cell Mol Med* 2010;14:771–94.
- Warburg O, Posener K, Negelein E. The metabolism of the carcinoma cell. In: Warburg O, ed. *The metabolism of tumors*. New York: Richard Smith, Inc.; 1931:29–169.
- Taizo Y, Yutaka S, Hirofumi F, et al. Over-expression of facilitative glucose transporter genes in human cancer. *Biochem Biophys Res Commun* 1990;170:223–30.
- Uchegbu IF. The biodistribution of novel 200 nm palmitoyl muramic acid vesicles. *Int J Pharm* 1998;162:19–27.
- Jianing Q, Ping Y, Fen H, et al. Nanoparticles with dextran/chitosan shell and BSA/chitosan core—doxorubicin loading and delivery. *Int J Pharm* 2010;393:176–84.
- Brownlie A, Uchegbu IF, Schatzlein AG. PEI-based vesicle-polymer hybrid gene delivery system with improved biocompatibility. *Int J Pharm* 2004;274:41–52.
- Vichai V, Kirtikara K. Sulforhodamine B colorimetric assay for cytotoxicity screening. *Nat Protoc* 2006;1:1112–16.
- Rao MV, Atreyi M, Rajeswar MR. Fluorescence studies on concanavalin-A. *J Biosci* 1984;6:823–8.
- Froehlich P. Understanding the sensitivity specification of spectrofluorometers. *Int Lab* 1989;19:42–5.
- Chipman DM, Grisaro V, Sharon N. The binding of oligosaccharides containing N-acetylglucosamine and N-acetylmuramic acid to lysozyme. The specificity of binding subsites. *J Biol Chem* 1967;242:4388–94.
- Wu G, Robertson DH, Brooks CL, Vieth M. Detailed analysis of grid-based molecular docking: a case study of CDOCKER-A CHARMM-based MD docking algorithm. *J Comput Chem* 2003;24:1549–62.
- Glide, version 5.8, Schrödinger, LLC, New York, NY; 2012.
- Maestro, version 9.3, Schrödinger, LLC, New York, NY; 2012.
- Okimoto N, Futatsugi N, Fuji H, et al. High-performance drug discovery: computational screening by combining docking and molecular dynamics simulations. *PLoS Comput Biol* 2009;5:1–12.
- Kandasamy R, Veinramuthu S. Formulation and optimization of zidovudine niosomes. *AAPS PharmSciTech* 2010;11:1119–27.
- You HB, Kinam P. Targeted drug delivery to tumors: myths, reality and possibility. *J Control Release* 2011;153:198–205.
- Sahin NO. Niosomes as nanocarrier systems. In: Mozafari MR, ed. *Nanomaterials and nanosystems for biomedical applications*. Netherlands: Springer; 2007:67–81.
- Al-Hamidi H, Edwards AA, Mohammad MA, Nokhodchi A. To enhance dissolution rate of poorly water-soluble drugs: glucosamine hydrochloride as a potential carrier in solid dispersion formulations. *Colloids Surf B* 2010;76:170–8.
- US2011/0243851. Glucose PEG conjugate for reducing glucose transport into the cell.
- Yamamoto T, Seino Y, Fukumoto H, et al. Over-expression of facilitative glucose transporter genes in human cancer. *Biochem Biophys Res Commun* 1990;170:223–30.
- Schlick KH, Lange CK, Gillispie GD, Cloninger MJ. Characterization of protein aggregation via intrinsic fluorescence lifetime. *J Am Chem Soc* 2009;131:16608–9.
- Sha Z, Shiladitya B, William C, et al. Leucine-aspartic acid-valine sequence as targeting ligand and drug carrier for doxorubicin delivery to melanoma cells: in vitro cellular uptake and cytotoxicity studies. *Pharmaceut Res* 2009;26:2578–87.
- Dorit G, Aviva TH, Dina T, et al. Nuclear delivery of doxorubicin via folate-targeted liposomes with bypass of multidrug-resistance efflux pump. *Clin Cancer Res* 2000;6:1949–57.
- Eksborg S. Extraction of daunorubicin and doxorubicin and their hydroxyl metabolites: self-association in aqueous solution. *J Pharm Sci* 1978;67:782–5.
- Mennozi M, Valentini L, Vannini E, Arcamone F. Self-association of doxorubicin and related compounds in aqueous solution. *J Pharm Sci* 1984;73:766–70.
- Takafumi M, Eriko T, Yuji K, et al. FDG uptake and glucose transporter subtype expressions in experimental tumor and inflammation models. *J Nucl Med* 2001;42:1551–5.
- Raffaele C, Agnese V, Cristina R, et al. Expression analysis of facilitative glucose transporters (GLUTs) in human thyroid carcinoma cell lines and primary tumors. *Mol Cell Endocrinol* 2008;291:57–62.
- Thomas AH, Robert BM, Richard AF, et al. Glide: a new approach for rapid, accurate docking and scoring. 2. Enrichment factors in database screening. *J Med Chem* 2004;47:1750–9.
- Friesner RA, Banks JL, Murphy RB, et al. Glide: a new approach for rapid, accurate docking and scoring. 1. Method and assessment of docking accuracy. *J Med Chem* 2004;47:1739–49.